

A semi-discrete high resolution scheme for nonlinear scalar conservation laws

Yousef Hashem Zahran

Abstract

The purpose of this paper is twofold. Firstly we carry out an extension of the fully discrete third order TVD scheme, for linear case, presented in [8] to nonlinear scalar hyperbolic conservation laws for one and two dimensions. Secondly, we propose a semi-discrete version of the scheme. Time evolution is carried out by the third order TVD Runge-Kutta method. The advantages of the scheme are its simplicity, third order, non-oscillatory and that can be used for large time steps which can save more time. Examples and convergence rates are presented for the Burger equation for one and two dimensions which confirm the high resolution content of the proposed schemes. We use exact solutions and other methods to validate the results.

Key words: Conservation laws, difference methods, TVD schemes, Burger equation, Runge-Kutta method.

1 Introduction

Hyperbolic conservation laws describe a variety of phenomena in several disciplines, such as physics, chemistry, environmental sciences and many others. Analytical solutions of the problems are available under very special circumstances and one thus has to rely on numerical methods for solving problems of practical interest. It is well known that the solutions of hyperbolic equations may develop discontinuities in finite time even if the initial condition is smooth. A major difficulty in the numerical approximation of nonlinear hyperbolic conservation laws is the presence of discontinuities in the solution. Traditional schemes generate spurious oscillations in the numerical solution near these discontinuities. Standard methods based on central differencing together with artificial viscosity have often been replaced, during the last few years, by the so-called total variation diminishing (TVD) schemes. The main property of a TVD scheme is that, unlike monotone schemes, it can be second order accurate (or higher) and oscillation-free across discontinuities (when applied to nonlinear equations).

A third order TVD finite difference scheme is presented in [8], which has so far been applied only to linear systems with constant coefficients. The scheme is conservative, one step, explicit and fully discrete, requiring only the computation of numerical fluxes to advance the solution by a full time step. In this paper we will present a generalization of the scheme for the case of nonlinear scalar case for one and two dimensions by using the technique in [7].

It is well known that the semi-discrete schemes are especially effective when they combine high resolution, non-oscillatory spatial discretisation with high order, large step size ordinary differential equation solvers for their time evolution.

In this paper we propose a semi-discrete version of the scheme with Runge-Kutta method for time discretisation. This scheme has the advantages of simplicity, third order, non-oscillatory and that can be used for large time steps which can save more time.

The paper is organized as follows. In section 2, we give a brief description of the third order TVD scheme for linear equations. In section 3 we describe the extension of the fully discrete scheme for nonlinear equations. In section 4 we construct the semi-discrete version of the scheme with Runge-Kutta method for time discretisation. Extension of the semi discrete scheme for two dimensions problems are presented in section 5. Numerical tests on the nonlinear equation with different initial conditions are performed in section 6. The numerical results are compared with exact solutions and other methods.

2 Third order fully discrete TVD scheme

In this section we review the fully discrete third order difference scheme presented in [8].

The initial value problem (IVP) for the one-dimensional scalar hyperbolic conservation law is considered, namely

$$u_t + f(u)_x = 0, \quad -\infty < x < \infty, \quad t \geq 0 \quad (2.1)$$

$$u(x, 0) = u_0(x) \quad (2.2a)$$

Here u is the unknown function and $f(u)$ is the physical flux.

First let us consider the linear case $f(u) = au$, so that $f'(u) = a$ is a constant wave propagation speed. If the initial data consists of two constant states,

$$u_0 = \begin{cases} u_L & x < 0 \\ u_R & x > 0 \end{cases} \quad (2.2b)$$

equation (2.1) with (2.2b) is called the usual Riemann problem (RP).

A uniform x - t grid, with mesh size Δx in the x -direction and Δt in the t -direction, is introduced with a fixed ratio $\lambda = \Delta t/\Delta x$. Let u_j^n denote the numerical solution obtained at $(x, t) = (j\Delta x, n\Delta t)$.

The third order conservation numerical scheme introduced in [8] has the form (for constant a)

$$u_j^{n+1} = u_j^n - \lambda \left[f_{j+1/2} - f_{j-1/2} \right] \quad (2.3)$$

with the numerical flux

$$f_{j+1/2} = \frac{1}{2} (au_j + au_{j+1}) - \frac{1}{2} |a| \Delta_{j+1/2} u + |a| \left\{ A_0 \Delta_{j+1/2} u + A_1 \Delta_{j+L+1/2} u + A_2 \Delta_{j+M+1/2} u \right\} \quad (2.4)$$

where

$$A_0 = \frac{1}{2} - \frac{|c|}{4}, \quad A_1 = -\frac{|c|}{8} - \frac{c^2}{8}, \quad A_2 = -\frac{|c|}{8} + \frac{c^2}{8} \quad (2.5)$$

$L = -1$, $M = 1$ for $c > 0$ and $L = 1$, $M = -1$ for $c < 0$, where $c = \lambda a$ is the Courant number and $\Delta_{j+1/2} u = u_{j+1} - u_j$.

The scheme is stable if and only if $|c| \leq \sqrt{2}$.

This scheme, being third order accurate scheme, is not TVD. It can be made TVD by replacing (2.4) with the more general form

$$f_{j+1/2} = \frac{1}{2} (au_j + au_{j+1}) - \frac{1}{2} |a| \Delta_{j+1/2} u + |a| \left\{ A_0 \Delta_{j+1/2} u + A_1 \Delta_{j+L+1/2} u \right\} \varphi_j + |a| A_2 \Delta_{j+M+1/2} u \phi_{j+M} \quad (2.6)$$

where ϕ_j and ϕ_{j+M} are flux limiter functions.

Theorem: Scheme (2.3) with (2.6) is TVD for $|c| \leq 1$ if the limiter function is determined by

$$\phi_j = \begin{cases} \frac{(1-|c|)\theta_j}{\eta(A_1\theta_j + A_0 - A_2)} & \text{for } 0 \leq \theta_j \leq \theta^L \\ 1 & \text{for } \theta^L \leq \theta_j \leq \theta^R \\ \frac{1-|c| + \eta A_2 \phi_{j+M} / \theta_j^*}{\eta(A_1\theta_j + A_0)} & \text{for } \theta_j > \theta^R \\ 0 & \text{for } \theta_j < 0 \end{cases} \quad (2.7a)$$

$$\phi_{j+M} = \begin{cases} \eta\theta_{j+M} & \text{for } 0 \leq \theta_{j+M} < 0.5 \\ 1 & \text{for } \theta_{j+M} > 0.5 \\ 0 & \text{for } \theta_j = 0 \end{cases} \quad (2.7b)$$

where $\theta^L = \frac{\eta(A_0 - A_2)}{1 - |c| - \eta A_1}$, $\theta^R = \frac{1 - |c| - \eta(A_0 - A_2 \phi_{j+M} / \theta_j^*)}{\eta A_1}$, and θ_j is called the local flow parameter and is defined by

$$\theta_j = \frac{\Delta_{j+L+1/2} u}{\Delta_{j+1/2} u} \quad (2.7c)$$

and θ_j^* is called the upwind-downward flow parameter and is given by

$$\theta_j^* = \frac{\Delta_{j+L+1/2} u}{\Delta_{j+M+1/2} u} \quad (2.7d)$$

and η is defined by

$$\eta = \begin{cases} 1 - |c| & \text{for } 0 \leq |c| < 1/2 \\ |c| & \text{for } 1/2 \leq |c| \leq 1 \end{cases} \quad (2.7e)$$

Proof : See [4] and [8].

3 Extension to nonlinear scalar hyperbolic conservation laws

In this section we extend the scheme (2.3) with (2.6) to nonlinear scalar problems

$$u_t + f(u)_x = 0, \quad (3.1)$$

For nonlinear equations the TVD procedure is empirical, but in practice it works very well as it will be demonstrated in the next sections. For more details see [4], [6] and [7]. Here we use the technique presented in [7]. Define the wave speed

$$a_{j+\frac{1}{2}} = \begin{cases} \frac{\Delta_{j+\frac{1}{2}} f}{\Delta_{j+\frac{1}{2}} u} & \Delta_{j+\frac{1}{2}} u \neq 0 \\ \left. \frac{\partial f}{\partial u} \right|_{u_j} & \Delta_{j+\frac{1}{2}} u = 0 \end{cases} \quad (3.2)$$

Now we redefine the θ_j in (2.7c) as

$$\theta_j = \frac{\left| a_{j+L+\frac{1}{2}} \right| \Delta_{j+L+\frac{1}{2}} u}{\left| a_{j+\frac{1}{2}} \right| \Delta_{j+\frac{1}{2}} u} \quad (3.3a)$$

and

$$\theta_j^* = \frac{\left| a_{j+L+1/2} \right| \Delta_{j+L+1/2} u}{\left| a_{j+M+1/2} \right| \Delta_{j+M+1/2} u} \quad (3.3b)$$

Here $c_{j+\frac{1}{2}} = \frac{\Delta t}{\Delta x} a_{j+\frac{1}{2}}$ is the Courant number.

Unlike the constant coefficient case, $a_{j+\frac{1}{2}}$ and $a_{j-\frac{1}{2}}$ are not always the same sign. Then the numerical flux (2.6) takes the form

$$\begin{aligned} f_{j+1/2} &= \frac{1}{2} (f_j + f_{j+1}) - \frac{1}{2} \left| a_{j+\frac{1}{2}} \right| \Delta_{j+1/2} u + \\ &\quad \left| a_{j+\frac{1}{2}} \right| \left\{ A_0 \Delta_{j+1/2} u + A_1 \Delta_{j+L+1/2} u \right\} \phi_j \\ &\quad + \left| a_{j+\frac{1}{2}} \right| A_2 \Delta_{j+M+1/2} u \phi_{j+M} \end{aligned} \quad (3.4)$$

After considering all the possible combinations of the signs of $a_{j+\frac{1}{2}}$ and $a_{j-\frac{1}{2}}$, a set of sufficient conditions on ϕ can still be of the form similar to (2.7) (see [8]) and is given by

$$\phi_j = \begin{cases} \frac{(1 - |a_{j+\frac{1}{2}}|)\theta_j}{\eta(A_1\theta_j + A_0 - A_2)} & \text{for } 0 \leq \theta_j \leq \theta^L \\ 1 & \text{for } \theta^L \leq \theta_j \leq \theta^R \\ \frac{1 - |a_{j+\frac{1}{2}}| + \eta A_2 \phi_{j+M} / \theta_j^*}{\eta(A_1\theta_j + A_0)} & \text{for } \theta_j > \theta^R \\ 0 & \text{for } \theta_j < 0 \end{cases} \quad (3.5a)$$

where

$$\phi_{j+M} = \begin{cases} \eta\theta_{j+M} & \text{for } 0 \leq \theta_{j+M} < 0.5 \\ 1 & \text{for } \theta_{j+M} > 0.5 \\ 0 & \text{for } \theta_j = 0 \end{cases} \quad (3.5b)$$

$$\text{where } \theta^L = \frac{\eta(A_0 - A_2)}{1 - |a_{j+\frac{1}{2}}| - \eta A_1}, \quad \theta^R = \frac{1 - |a_{j+\frac{1}{2}}| - \eta(A_0 - A_2 \phi_{j+M} / \theta_j^*)}{\eta A_1}$$

where θ_j and θ_j^* are defined in (3.3).

Observe that when $a_{j+\frac{1}{2}} = 0$, the scheme has zero dissipation. One way is to approximate $a_{j+\frac{1}{2}}$ by a Lipschitz continuous function [2]. For example, instead of using (3.4), one can use

$$\begin{aligned} f_{j+1/2} &= \frac{1}{2}(f_j + f_{j+1}) - \frac{1}{2}\psi(a_{j+\frac{1}{2}})\Delta_{j+1/2}u \\ &+ \psi(a_{j+\frac{1}{2}})\left\{A_0\Delta_{j+1/2}u + A_1\Delta_{j+L+1/2}u\right\}\phi_j \\ &+ \psi(a_{j+\frac{1}{2}})A_2\Delta_{j+M+1/2}u\phi_{j+M} \end{aligned} \quad (3.6)$$

Here ψ is a function of $a_{j+\frac{1}{2}}$ and is defined as

$$\psi(x) = \begin{cases} \frac{x^2}{4\varepsilon} + \varepsilon & \text{for } |x| < 2\varepsilon \\ |x| & \text{for } |x| \geq 2\varepsilon \end{cases} \quad \text{where } 0 \leq \varepsilon \leq 0.5.$$

For the third order TVD scheme the linear stability condition reads $CFL \leq 1$. Here CFL denotes the maximum Courant number over all cells at a given time step:

$$CFL = \max(S_j^n \frac{\Delta t}{\Delta x})$$

where S_j^n is the maximum propagation speed at time level n .

4 Semi-discrete formulation

Another way to discretize (2.1) is to keep the time variable t continuous and consider semi-discrete scheme

$$\frac{d}{dt}(u_j(t)) = -\frac{1}{\Delta x} \left[f_{j+\frac{1}{2}} - f_{j-\frac{1}{2}} \right] = L_j(u) \quad (4.1)$$

where $f_{j+\frac{1}{2}}$ is defined in (3.6).

The time discretisation will be implemented by a third order TVD Runge-Kutta method developed in [1].

This Runge-Kutta method is used to solve a system of initial value of ordinary differential equations written as

$$\frac{du}{dt} = L(u), \quad (4.2)$$

where $L(u)$ is an approximation to the derivative $(-f(u)_x)$ in the differential equation (2.1).

In [1], schemes up to third order were found to satisfy the TVD conditions. The optimal third order TVD Runge-Kutta method is given by

$$\begin{aligned} u^{(1)} &= u^n + \Delta t L(u^n) \\ u^{(2)} &= \frac{3}{4}u^n + \frac{1}{4}u^{(1)} + \frac{1}{4}\Delta t L(u^{(1)}) \\ u^{n+1} &= \frac{1}{3}u^n + \frac{2}{3}u^{(2)} + \frac{2}{3}\Delta t L(u^{(2)}) \end{aligned} \quad (4.3)$$

In [1], it has been shown that, even with a very nice second order TVD spatial discretization, if the time discretization is by a non-TVD but linearly stable Runge-Kutta method, the result may be oscillatory. Thus it would always be safer to use TVD Runge-Kutta methods for hyperbolic problems.

5 Extension to multidimensional problems

The present schemes can be applied to multidimensional problems by means of space operator splitting. The original idea is attributed to Strang [5]. As an example we consider the two dimensional Burger equation

$$U_t + [F(U)]_x + [G(U)]_y = 0 \quad (5.1)$$

where $F(U) = G(U) = \frac{1}{2}U^2$

There are several versions of space splitting. Here we take the simplest one, whereby the two dimensional problem (5.1) is replaced by the sequence of two one-dimensional problems

$$U_t + [F(U)]_x = 0 \quad (5.2a)$$

$$U_t + [G(U)]_y = 0 \quad (5.2b)$$

If the data U^n at time level n for problem (9.1) are given, the solution U^{n+1} at time level $n+1$ is obtained in the following two steps:

- a) solve equation (5.2a) with data U^n to obtain an intermediate solution \bar{U}^{n+1} (x -sweep);
- b) solve equation (5.2b) with data \bar{U}^{n+1} to obtain the complete solution U^{n+1} (y -sweep);

For three dimensional problems there is an extra z -sweep.

6 Numerical experiments

In this section we present the results of our numerical experiments for the fully discrete third order TVD scheme (2.3) with (3.6) and semi-discrete scheme (4.1). for time evolution we use the third order Runge-Kutta method (4.3) reviewed and developed in the previous section. We compare these methods with the third order finite difference scheme presented in [3].

We compare the following schemes:

1. LT3 : the fully discrete third order presented in [3].
2. TVD3 : the fully discrete third order scheme (2.3) with (3.6).
3. STVD3 : the semi-discrete scheme (4.1) with (4.3).

For each scheme we select a value of CFL that satisfies the stability condition: LT3 scheme has CFL = 0.33 and the other schemes CFL= 0.8.

6.1 Accuracy test

Example 1: We solve the nonlinear scalar Burger equation

$$u_t + \left[\frac{1}{2}u^2\right]_x = 0 \quad (6.1)$$

subject to two periodic initial data

$$u_0(x) = 1 + 0.5 \sin(\pi x) \quad (6.2)$$

on $[-1, 1]$. When $t = \frac{1}{\pi}$ the solution is still smooth, and the errors and numerical orders of accuracy are shown in Table 1. It can be seen that STVD3 scheme is the most accurate and it is less expensive because it enjoys a less restrictive CFL condition ($\lambda = 0.8$ versus $\lambda = 0.33$). Comparing the magnitudes of the errors with the results obtained with LT3 and TVD3, we note that our new scheme STVD3 scheme yields smaller errors than the others.

6.2 Test cases with shocks

Example 2: We solve the Burger equation (5.1) with periodic initial condition

$$u_0(x) = 0.5 + \sin(\pi x) \quad (6.3)$$

We plot the results at time $t = \frac{1.5}{\pi}$ when the shock has already appeared in the solution. In Figure 1 the solutions of LT3 method (a), TVD3 (b) and STVD3 (c) with 100 grid points are shown. The solid line is the exact solution and symbols are the numerical solutions.

Note that the results obtained by LT3 are satisfactory while the results by TVD3 are better. The solutions obtained by STVD3 scheme are almost indistinguishable from exact solutions.

Example 3: We solve (6.1) with initial condition

$$u(x, 0) = \begin{cases} -1 & |x| \geq 0.5 \\ 2 & |x| < 0.5 \end{cases} \quad (6.4)$$

The breakdown of the initial discontinuity results in a shock wave with speed 0.5 and a rarefaction with a sonic point at $x = 0.5$. The exact solution consists of rarefaction wave (left) and shock wave (right). At $t = 2/3$ the rarefaction hits the shock and then the solution has a rarefaction wave only. Using $x = 0.01$. The numerical solution is displayed at $t = 0.4$ (before collision of the head of the rarefaction with the shock) and $t = 1.1$ (after collision). Results are shown in Figures 2 and 3 respectively, where the numerical solutions, shown by symbols, are compared with the exact solution, shown by a full line. Figure 2 shows the computed results at $t = 0.4$ using LT3, TVD3 and STVD3 schemes and Figure 3 shows the results at $t = 1.1$. Notice that the numerical solution obtained by STVD3 are indistinguishable from exact solutions.

Example 4: We finally show the results obtained with Burger's equation in Figure 4. The initial condition is $U_0(x, y) = \sin^2(\pi x) \sin^2(\pi y)$ on $(0, 1) \times (0, 1)$. We consider periodic boundary conditions. Figure 4 shows the results at $t = 2$ using TVD3 method (left) and STVD3 method (right). Also Figure 5 shows the results at $t = 4$ using TVD3 (left) and STVD3 (right). We note, from the figures 4 and 5, lack of spurious oscillations while the shocks are well resolved.

References

- [1] S. Gottlieb and C.W. Shu, Total variation diminishing Runge-Kutta schemes, *Math.comp.* 67(1998) pp.73-85.
- [2] Harten, A., High resolution schemes for hyperbolic conservation laws, *J. Comput. Phys.* 49(1983) pp 357-393.
- [3] Liu X.D. and Tadmor E. Third order non-oscillatory central scheme for hyperbolic conservation laws *J. Numer.Math.*, 79(1998) pp. 397-425.
- [4] Shi J. and Toro E.F., Fully discrete high order shock capturing numerical schemes, *Int.J.Numer.Methods fluids*,23(1996) pp 241-269.
- [5] Strang, G. On the construction and comparison of finite difference schemes *SIAM J. Numer. Anal.*5 (1968) pp.506-517.
- [6] Toro E.F. A weighted average flux methods for hyperbolic conservation laws *Proc.R.Soc.Lond.A.*(1989) pp 401-418.
- [7] Yee H.C. Construction of explicit and implicit symmetric TVD schemes and their applications *J. Comput. Phys.* 68 (1987) pp. 151-179.
- [8] Yousef H. Zahnran Third order TVD scheme for hyperbolic conservation laws *J. Application of Mathematics* (accepted for publication).

| N | LT3 | | TVD3 | | STVD3 | |
|-----|-------------|-------------|-------------|-------------|-------------|-------------|
| | L^1 error | L^1 order | L^1 error | L^1 order | L^1 error | L^1 order |
| 80 | 0.4281E-4 | | 0.5492E-4 | | 0.1799E-4 | |
| 160 | 0.5282E-5 | 2.87 | 0.6908E-5 | 2.991 | 0.2229E-5 | 3.0125 |
| 320 | 0.9049E-6 | 2.69 | 0.9820E-6 | 2.814 | 0.2774E-6 | 3.0065 |
| 640 | 0.1591E-6 | 2.51 | 0.1621E-6 | 2.599 | 0.3463E-7 | 3.0020 |

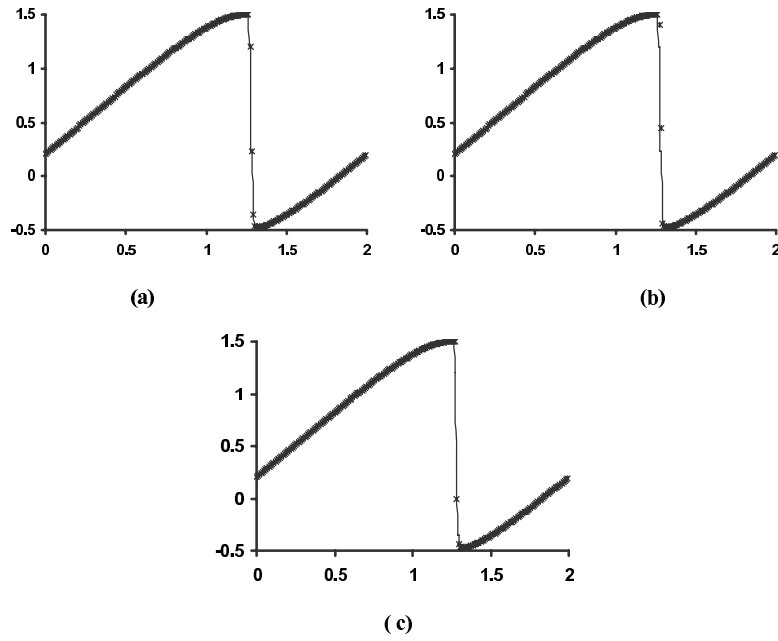


Figure 1: Solution of example 2 by LT3 scheme (a) TVD3 scheme (b) and STVD3 scheme (c).

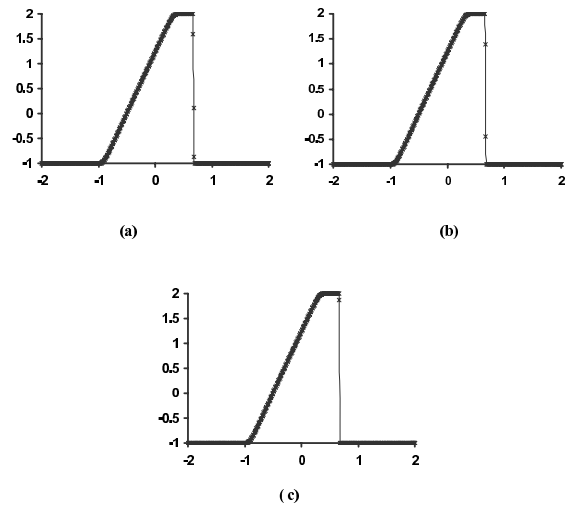


Figure 2: Solution of example 3 at $t = 0.4$ by LT3 scheme (a), TVD3 scheme (b) and STVD3 scheme (c).

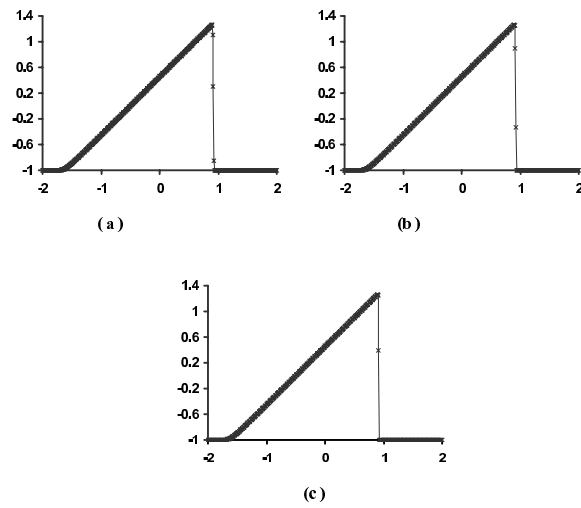


Figure 3: Solution of example 3 at $t = 1.1$ by LT3 scheme (a), TVD3 (b) and STVD3 scheme (c).

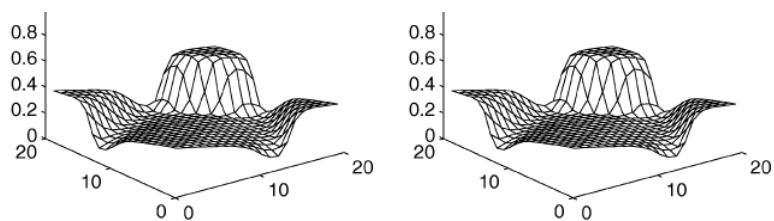


Figure 4: The solution of two dimensional equation at $t = 2$ using TVD3 (left) and STVD3 (right) methods.

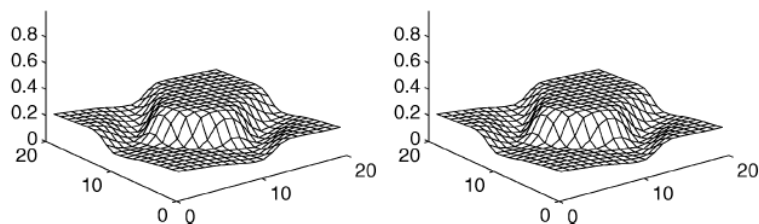


Figure 5: The solution of two dimensional equation at $t = 4$ using TVD3 (left) and STVD3 (right) methods.

YUSEF HASHEM ZAHRAN
PHYSICS AND MATHEMATICS DEPARTMENT
FACULTY OF ENGINEERING, PORT SAID, EGYPT